P2.4 THE 3D EQUILIBRATION OF A BAROCLINIC JET: POTENTIAL MOMENTUM DIAGNOSTICS

Pablo Zurita-Gotor*
SUNY Stony Brook, Stony Brook, New York
R.S. Lindzen
MIT, Cambridge, Massachusetts

1. INTRODUCTION

In an accompanying poster (poster P2.6, P2.6 hereafter), we discuss the equilibration of the 3D Charney problem, emphasizing the redistribution of momentum and the maintenance of the momentum balance. It is shown in that paper that the momentum flux plays an important role in the equilibration. We also introduced in section 4.2 (S4.2 hereafter) a momentum-based formalism, in which the thermal field is encapsulated as 'potential' momentum. In this work, we apply that formalism to the 3D baroclinic equilibration problem described above, which supports and complements the results of P2.6.

2. THEORY

The concept of potential momentum was introduced in S4.2 and is succinctly reviewed here. The potential momentum M is the zonal momentum profile that gives the same PV distribution as the stretching term in the full 3D basic state. Mathematically:

$$M = -\int_0^y \frac{\partial}{\partial z}\left(\frac{f_0}{\Theta_z}\theta\right) dy' \qquad (1)$$

where $\Theta(z)$ is the reference temperature profile of qg theory, which we can define so that $\overline{\theta}_z$ integrates meridionally to zero. Physically, easterly (westerly) potential momentum is associated to isentropic layers that open up (close down) with latitude.

This definition is also extrapolated to the surface:

$$M_s(y,z) = -\frac{f_0}{\Theta_z}\int_0^y (\theta - \Theta_0)\,\delta(z)dy' \qquad (2)$$

where Θ_0 is the mean surface temperature. A negative surface temperature gradient is thus equivalent to a delta-function easterly potential momentum jet.

The adiabatic rearrangement of mass within the isentropic layers, approximated in qg-theory by the residual circulation $\overline{v}^*$, exchanges potential and physical momentum. A poleward circulation $\overline{v}^*$ generates easterly potential momentum $\overline{M}$ in the interior by concentrating the isentropic mass poleward, and also generates westerly physical momentum $\overline{U}$ via the Coriolis force. However, it does not change the total momentum $\overline{M}+\overline{U}$, as described mathematically by the following set of equations[1]:

$$\frac{\partial \overline{U}}{\partial t} - f_0\overline{v}^* = \overline{v'q'} - \alpha_M\overline{U} \qquad (3)$$

$$\frac{\partial \overline{M}}{\partial t} + f_0\overline{v}^* = -\alpha_T(\overline{M} - \overline{M}_R) \qquad (4)$$

$$\frac{\partial}{\partial t}\left(\overline{M}+\overline{U}\right) = \overline{v'q'} - D_{mean} \qquad (5)$$

$$\frac{\partial}{\partial t}\overline{A} = -\overline{v'q'} - D_{eddy} \qquad (6)$$

Equations 3-5 imply that the residual circulation $\overline{v}^*$ only affects the partition between $\overline{M}$ and $\overline{U}$, but not the net mean momentum. The net mean momentum $\overline{M}+\overline{U}$ can only be changed through the eddy drag $\overline{v'q'}$ (i.e., wave-mean flow interaction generating pseudomomentum $\overline{A}$ at the expense of the mean flow momentum) and/or dissipation. The residual circulation only exchanges both forms of mean momentum, so as to enforce thermal wind balance:

$$\frac{\partial^2 \overline{M}}{\partial y^2} = \frac{\partial}{\partial z}\left(\frac{f_0^2}{N^2}\frac{\partial \overline{U}}{\partial z}\right), \qquad (7)$$

which implies that, when $\overline{M}$ varies in horizontal scales of the order of the deformation radius, the interior jets of physical and potential momentum should be of the same order. Finally, note that the 2D mixing depth constraint of P2.6 implies that the vertically integrated $\overline{M}$ is constant. All the terms in equation 4 integrate independently to zero and only redistribute potential momentum vertically.

General circulation

The general circulation can be described as follows:

1) Diabatic processes generate easterly potential momentum at lower levels, and compensating westerly potential momentum aloft. In particular, they force

* Corresponding author address: Pablo Zurita-Gotor, ITPA/MSRC, SUNY Stony Brook, Stony Brook, NY 11794-5000; email: pzurita@alum.mit.edu.

[1] See S2.4 for the explicit expressions of D_{mean} and D_{eddy}

the surface temperature gradient, which can be interpreted as a surface reservoir of easterly potential momentum. This also gives a negative delta PV gradient and supports baroclinic instability.

2) The growth of the baroclinic waves yields downgradient PV fluxes, whence easterly (westerly) eddy drag in the interior (at the surface). The surface has no mass and is subject to no net acceleration: the westerly eddy drag must be exactly balanced by the Coriolis force acting on the equatorward branch of the residual circulation. This term produces an easterly $\overline{U}$ tendency at the expense of depleting the potential momentum reservoir at the surface.

3) The interior branch of this poleward circulation transforms westerly potential to physical momentum in the interior. This westerly acceleration is balanced by the combined easterly drag of the eddy PV flux and surface friction. The system reaches an equilibrium when the diabatic generation of westerly potential momentum in the interior is balanced by the total easterly drag, and both are equal to the rate of conversion by the residual circulation.

This equilibrium is modeled by equations 3, 4 when the time derivatives are dropped:

$$\alpha_T \left(\overline{M} - \overline{M}_R\right) = -f_0 \overline{v}^* = \overline{v'q'} - \alpha_M \overline{U} \qquad (8)$$

The left hand side gives the diabatic generation of potential momentum and the right hand side the net momentum drag. In equilibrium, both must be equal, and also equal to the rate of conversion from $\overline{M}$ to $\overline{U}$ by the residual circulation. Hence,

$$\frac{f_0}{\Theta_z} \int_0^y \left(\overline{\theta}_S - \overline{\theta}_{RS}\right) dy' = -\int_0^{0^+} \left(\overline{M} - \overline{M}_R\right) dz =$$

$$= \int_{0^+}^{\infty} \left(\overline{M} - \overline{M}_R\right) dz = \frac{1}{\alpha_T} \left[-\alpha_M \delta \overline{U}_S + \int_{0^+}^{\infty} \overline{v'q'} dz\right]$$

which relates the thermal imbalance at the surface to the net interior drag. We assumed above that friction is limited to a surface layer of depth δ.

The eddy PV flux also gives the rate of generation of pseudomomentum, that must be balanced in equilibrium by eddy enstrophy dissipation (equation 6):

$$\overline{v'q'} = -D_{eddy} \approx -\frac{1}{\overline{q}_y} \left(\alpha_M \overline{\xi' q'} - \alpha_T \overline{m'_y q'}\right) \qquad (9)$$

Neglecting the mechanical dissipation in the free troposphere, we are then left with the simple balance:

$$\alpha_T \left(\overline{M} - \overline{M}_R\right) \overline{q}_y \approx \alpha_T \overline{m'_y q'}, \qquad (10)$$

in which the diabatic time scale disappears. This is an extension of the enstrophy constraint of Schoerberl and Lindzen (1984). It simply reflects the fact that the same time scale is responsible for the forcing of the zonal mean temperature gradient and for the diabatic damping of the temperature perturbations. When the mechanical dissipation is small, there can be no vertical motion and no generation of mechanical energy[2]. In that limit, the Lagrangian heat balance is trivial, $\overline{Q}^L = 0$: on average, the air parcels warm up as much when they are displaced equatorward of their equilibrium positions as they cool when they move poleward.

In the limit in which equation 10 is approximately valid, both the diabatic and frictional time scale disappear. However, this does *not* imply that the equilibrium state is insensitive to these time scales. A local balance as represented by 8 and 10 only applies for the equilibrated system. The time-dependent adjustment on the other hand is non-local, and may depend on the diabatic and frictional time scales in a non-trivial way. For instance, we will show that in the equilibrated state of our model the interior drag is dominated by $\overline{v'q'}$, while surface friction only makes up for a small fraction. However, one should be careful not to infer from this that the equilibrium state is insensitive to friction. Indeed, note that:

$$\int_{0^+}^{\infty} \left(f_0 \overline{v}^* + \overline{v'q'}\right) dz = -\int_0^{\infty} \frac{\partial}{\partial y} \overline{u'v'} dz > 0, \quad (11)$$

which implies that the easterly eddy drag alone is not strong enough to balance the net conversion of potential to physical momentum in the interior.

This is consistent with the findings of P2.6 that, without friction, there is a sustained acceleration of the jet. This result is of course already transparent in the original Eulerian framework, in which the eddy momentum flux is unbalanced. However, our formalism also explains why this is accompanied by the elimination of the surface temperature gradient, as the barotropic acceleration of the jet ultimately occurs at the expense of the surface potential momentum, which is depleted in the absence of friction.

3. MODEL RESULTS

We next show some diagnostics for the same runs described in P2.6. The model used is a Charney-Boussinesq model, in which the vertical shear Λ is also modulated meridionally with a Gaussian envelope. Newtonian cooling with a time scale of 20 days relaxes the temperature field to this 'radiative equilibrium' profile, and Rayleigh damping of varying time scale is used at the lowest resolved level alone.

[2] In reality, small scale dissipation is inevitable to absorb the enstrophy cascade resulting from the baroclinic source.

The runs described in P2.6 explore the sensitivity of the equilibrated state to namely two parameters: the frictional time scale τ and the dimensionless depth of the mode H/h (changed in our model by changing β). In the 2D case, the available interior PV gradient (i.e., the depth of the mode) limits the adjustment in vertical shear, and thus the maximum reduction in the surface temperature gradient. However, this is no longer a constraint in the 3D problem, in which the interior PV gradient is also enhanced through the development of horizontal curvature by the convergent eddy momentum fluxes. It is argued in P2.6 that to the extent that friction limits the development of the horizontal curvature, it also limits the reduction in vertical shear.

In this section, we look at those results from a potential momentum viewpoint. Because $\overline{\theta}_z = 0$, the interior potential momentum of the chosen basic state is zero, and all the potential momentum is initially locked at the surface. However, this is no longer the case for the equilibrated flow. Figure 1 shows some results for the run with $\beta = 3.0 \times 10^{-11} m^{-1} s^{-1}$ ($H/h = 1.6$) and frictional time scale 1 day. Panel A shows the potential momentum field and panel B the zonal wind, with the isentropic distribution also shown overlaid. As can be seen, the equilibrated flow has developed easterly $\overline{M}$ in the interior, as the isentropic layers open up with latitude[3] (panel C).

As discussed above, the generation of this interior easterly potential momentum jet occurs at the expense of the depletion of the surface potential momentum. This is illustrated in panel D, in which we show the vertically integrated potential momentum in the interior (thick solid) and at the surface, both initially (dashed) and at equilibration (thin solid). The integrated potential momentum in the interior exactly balances the deficit at the surface from radiative equilibrium. Finally, panels E-F demonstrate that, away from the boundary layer, the system reaches an equilibrium in which the diabatic generation of westerly potential momentum is exactly balanced by the easterly eddy drag (equation 8).

Note that the physical and potential momentum jets have comparable strength, as required by the thermal wind constraint. Hence, the horizontal and vertical curvature PV gradients are comparable, which is ultimately the reason why the 2D mixing depth constraint does not apply (see P2.6). This is best understood in a potential momentum framework, in which $\overline{q}_y = \beta - \partial_{yy}(\overline{M} + \overline{U})$. The reason why the generation of interior easterly $\overline{M}$ is not limited by β is because the compensating generation of westerly $\overline{U}$ (equations 3, 4) prevents a negative $\overline{q}_y$.

[3]But note that the isentropic slope is large, and the thickness varies much less along the isentropes than horizontally.

Sensitivity to friction

Figure 2 shows the results for a run with the same parameters but reduced surface friction (5 days). Not surprisingly, the flow equilibrates in this case by developing a stronger barotropic jet. A more remarkable difference, however, is that the surface shear is also reduced from the previous case. This was already noted in P2.6, but the connection is most transparent in the potential momentum framework. In this framework, the barotropic acceleration of the jet results from a conversion from $\overline{M}$ to $\overline{U}$ in the interior, while the conservation of the vertically-integrated potential momentum demands that this be accompanied by a westerly potential momentum acceleration at the surface, i.e., by a reduction of the surface temperature gradient. Panels C and D show that, indeed, the partition between surface and interior $\overline{M}$ is shifted to the interior in this case.

Figure 3 compares the vertically-integrated (excluding delta surface contributions) balance of total momentum at the center of the channel for the high and low friction cases. As can be seen, friction has in both cases a very small contribution, so that the equilibrium state essentially reflects a balance between diabatic forcing and eddy drag. Yet in a subtle way the final equilibrium is controlled by friction: because the eddy drag cannot balance by itself the $\overline{M}$ to $\overline{U}$ conversion (equation 11), friction is what ultimately limits the release of the surface potential momentum. When friction is small this conversion is more active, which results in a larger eddy drag and a larger generation of eddy pseudomomentum $\overline{A}$ (rather than in a larger $\overline{U}$ sink).

The important role played by friction is summarized in figure 4, which shows results for a number of runs with $H/h = 0.86$ and varying frictional time scale. The left panels show the partition between the surface and interior potential momentum. As friction is increased, the vertical redistribution of potential momentum is inhibited and the eddies are less efficient in reducing the surface temperature gradient. This also results in weaker interior jets for both $\overline{M}$ and $\overline{U}$. In fact, the $\overline{M}$ and $\overline{U}$ jets are comparable in all cases (as demanded by the thermal wind constraint), both being stronger with weaker friction.

Acknowledgments: This research is part of the thesis work of P.Z. at MIT. We acknowledge support by NSF Grant ATM-9421195 and DOE Grant FG02-93ER61673.

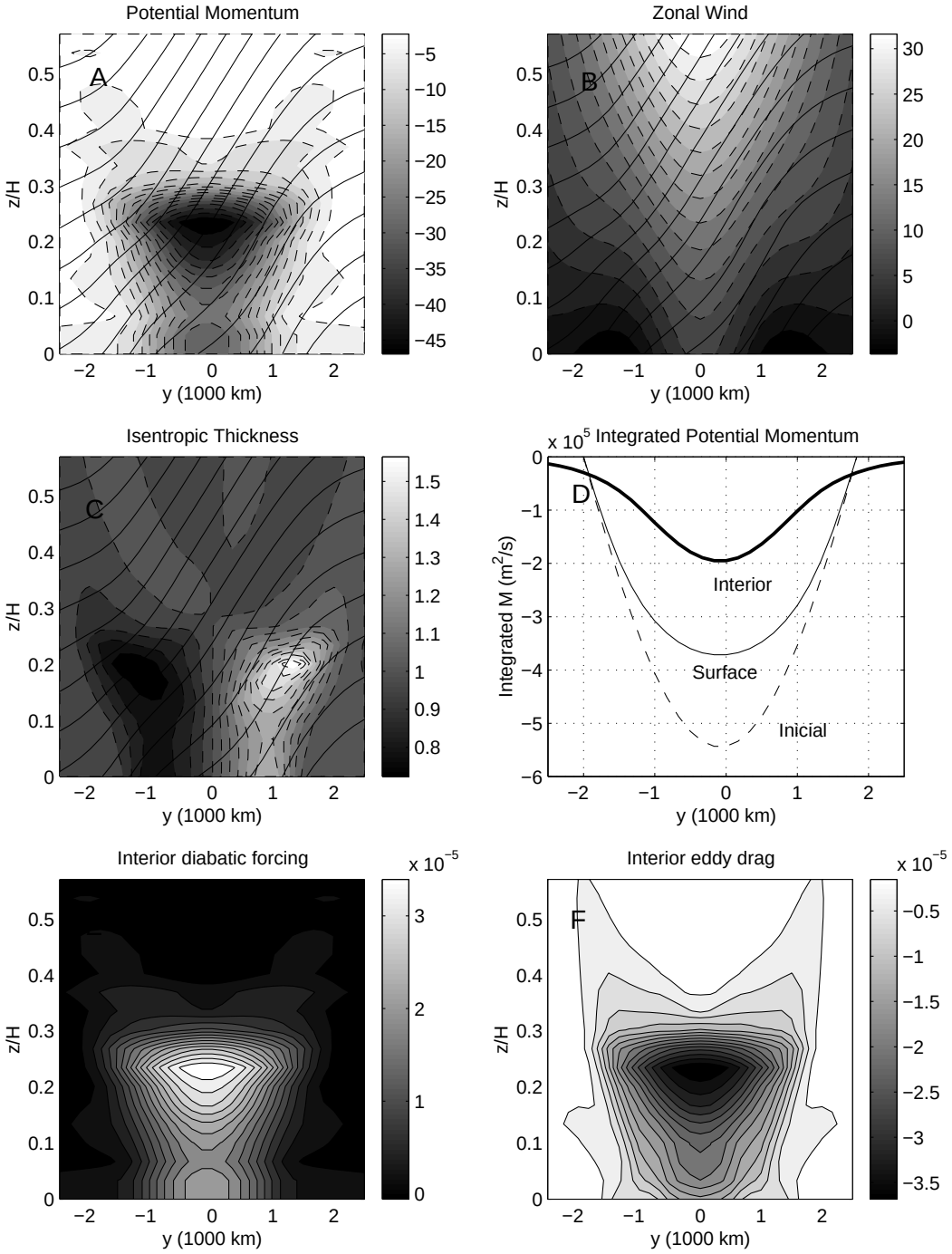

Figure 1: *Potential momentum diagnostics for the run with* $\beta = 3.0 \times 10^{-11}\ m^{-1}s^{-1}$ *(*$H/h = 1.6$*) and friction time scale 1 day: (A) Interior potential momentum (in m/s) (B) Zonal wind (C) Isentropic thickness, normalized by the reference thickness(D) Vertically integrated potential momentum at the surface (thin solid), in the interior (thick solid), and at the surface in radiative equilibrium (dashed) (E) Diabatic forcing of potential momentum in the interior, in* m/s^2 *(F) Interior eddy drag* $\overline{v'q'}$ *in* m/s^2*. In panels A-C the isentropes are also shown overlaid.*

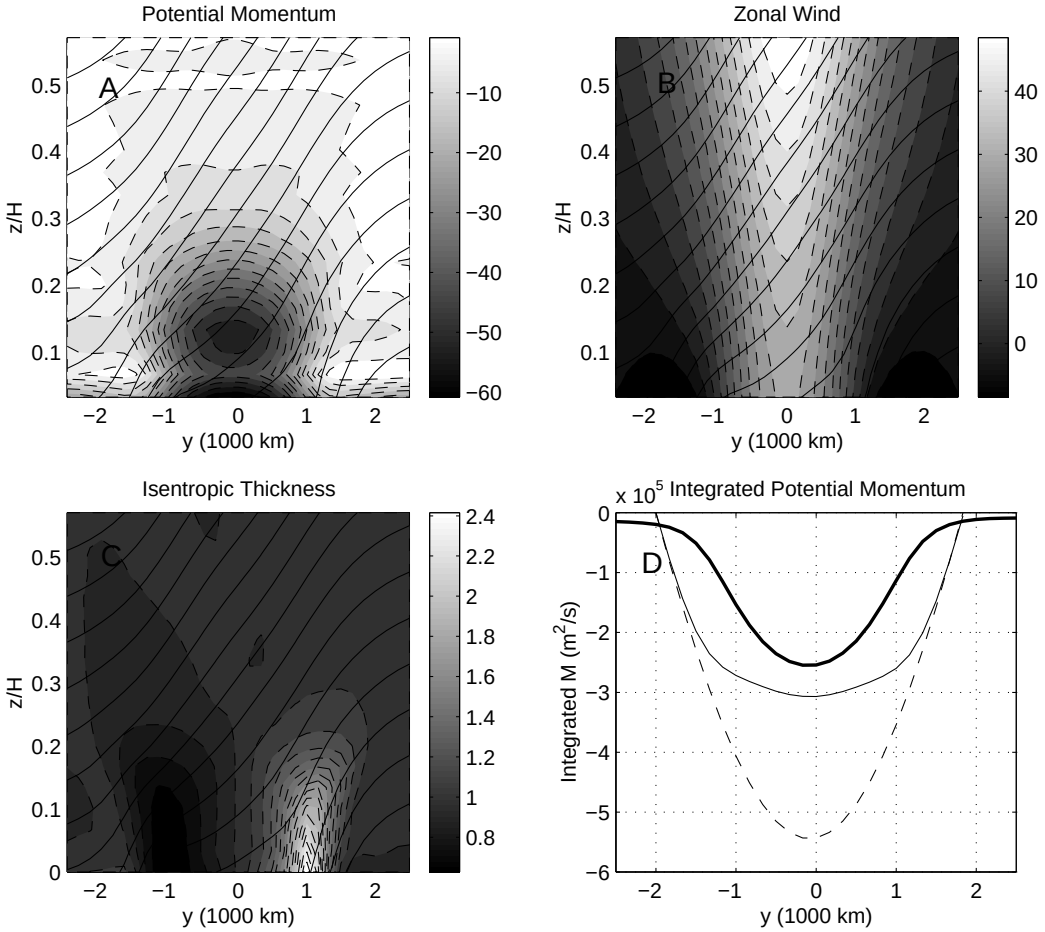

Figure 2: *As figure 1 but for the run with* $\beta = 3.0 \times 10^{-11}\ m^{-1}s^{-1}$ *(*$H/h = 1.6$*) and friction 5 days.*

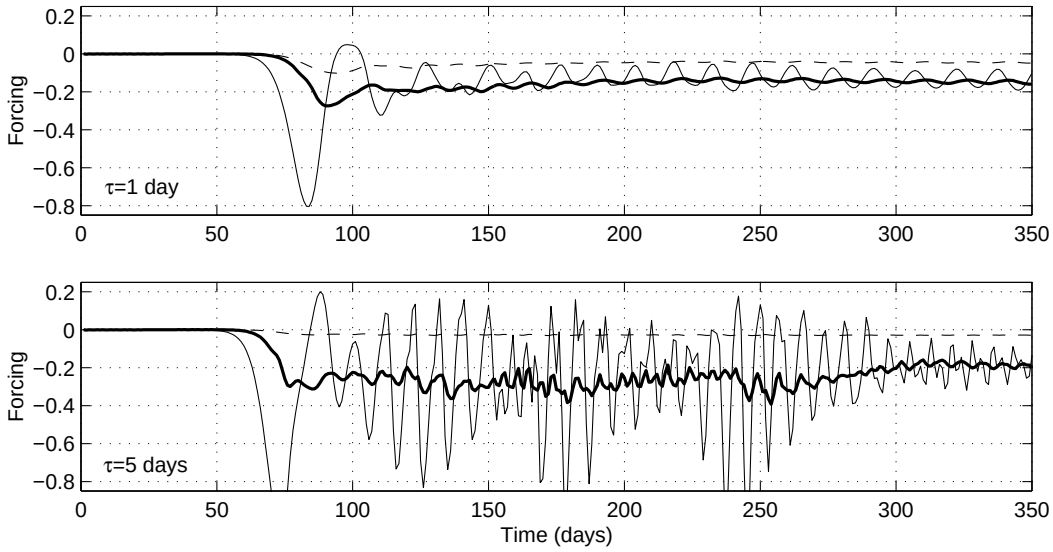

Figure 3: *Time series of the different contributions to the interior forcing of total momentum, vertically integrated at the center of the channel: diabatic (thick solid), eddy drag (thin solid) and frictional (dashed) for the runs with* $\beta = 3.0 \times 10^{-11}\ m^{-1}s^{-1}$ *(*$H/h = 1.6$*) and the frictional time scales indicated.*

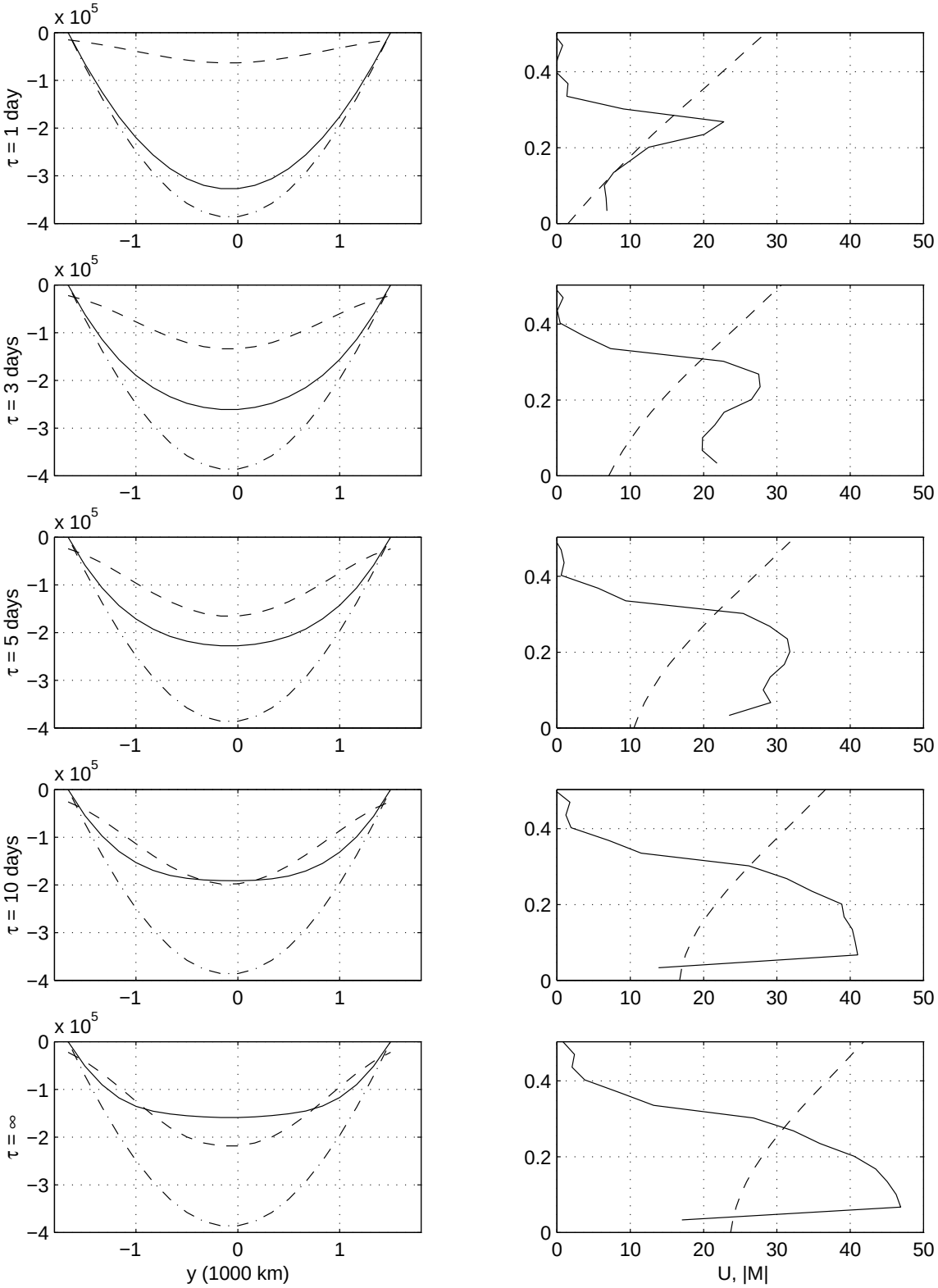

Figure 4: *For the runs with $\beta = 1.6 \times 10^{-11}\ m^{-1}s^{-1}$ $(H/h = 0.86)$ and the frictional time scales indicated: (Left) Integrated potential momentum in the interior (dashed), at the surface (solid), and in radiative equilibrium (dash-dotted). (Right) Vertical profiles of zonal mean flow (dashed) and (easterly) potential momentum (solid) at the center of the channel.*